

Lawrence Berkeley National Laboratory

Recent Work

Title

PRODUCTION OF π^+ PHOTO MESONS AS A FUNCTION OF ATOMIC NUMBER

Permalink

<https://escholarship.org/uc/item/55j9x9tt>

Author

Mozley, Robert F.

Publication Date

1950-05-29

cy 2

UNIVERSITY OF CALIFORNIA - BERKELEY

TWO-WEEK LOAN COPY

*This is a Library Circulating Copy
which may be borrowed for two weeks.
For a personal retention copy, call
Tech. Info. Division, Ext. 5545*

RADIATION LABORATORY

DISCLAIMER

This document was prepared as an account of work sponsored by the United States Government. While this document is believed to contain correct information, neither the United States Government nor any agency thereof, nor the Regents of the University of California, nor any of their employees, makes any warranty, express or implied, or assumes any legal responsibility for the accuracy, completeness, or usefulness of any information, apparatus, product, or process disclosed, or represents that its use would not infringe privately owned rights. Reference herein to any specific commercial product, process, or service by its trade name, trademark, manufacturer, or otherwise, does not necessarily constitute or imply its endorsement, recommendation, or favoring by the United States Government or any agency thereof, or the Regents of the University of California. The views and opinions of authors expressed herein do not necessarily state or reflect those of the United States Government or any agency thereof or the Regents of the University of California.

Copy D

UCRL 706

Production of π^+ Photo-mesons as
a Function of Atomic Number

By

Robert Fred Mozley
A.B. (Harvard University) 1938

DISSERTATION

Submitted in partial satisfaction of the requirements for the degree of

DOCTOR OF PHILOSOPHY

in

Physics

in the

GRADUATE DIVISION

of the

UNIVERSITY OF CALIFORNIA

Approved:

.....
.....
.....

Committee in Charge

Deposited in the University Library.....

Date

Librarian

Table of Contents

	Page
List of Illustrations	3
I Introduction	4
II General Description of Experiment	5
III Discussion of the Method	6
1. Use of μ^+ Meson Decay for the Detection of π^+ Mesons	6
2. Analysis of Error Caused by π^- and π^+ Mesons Decaying in Flight	8
3. Other Possible Causes of a 2 Microsecond Mean Life	11
IV Experimental Details	12
1. Methods for Reducing Background	12
2. X-ray Spectrum	13
3. Integration of X-ray Beam	15
4. Detection Equipment	15
5. Background Measurement	16
6. Stability of the Electronic Equipment	17
7. Design of Targets	18
8. Scattering of Mesons in Absorber	20
9. Computation of Energies and Relative Cross Sections	21
V Results of the Experiment	22
1. Data of a Typical Graphite Run	22
2. Summary of Data	23
3. Corrections	27
4. Relative Cross Sections	29
5. Estimate of Error	32
VI Discussion of Results	33
Acknowledgements	36
References	37

List of Illustrations

- Fig. 1 Synchrotron and Shielding for Meson Detection Telescope.
- Fig. 2 Arrangement of Target, Absorbers, and Meson Detection Telescope.
- Fig. 3 Time Variation of Magnetic Field of Synchrotron and X-ray Beam Intensity.
- Fig. 4 Bremsstrahlung Distribution from Synchrotron.
- Fig. 5 Block Diagram of Electronics.
- Fig. 6 Wave Shapes in Electronics.
- Fig. 7 Electronic Equipment.
- Fig. 8 Meson Counting Rate and Counting Rate of Pulses from Crystal I as a Function of Channel I Gain.
- Fig. 9 Meson Counting Rate and Counting Rate of First Pulse from Crystal II as a Function of Channel IIA Gain.
- Fig. 10 Meson Counting Rate and Counting Rate of 2nd Pulse from Crystal II as a Function of Channel IIB Gain.
- Fig. 11 Targets.
- Fig. 12 Relative Cross Sections for Production of π^+ Mesons by X-rays from Synchrotron.
- Fig. 13 Relative Cross Sections for Production of π^+ Mesons with $\frac{1}{A^{1/3}}$ Curves Superimposed, Normalized at Carbon.

Production of π^+ Photo-mesons as
a Function of Atomic Number

Robert F. Mozley

I Introduction

A measurement of the cross section for the production of π^+ photo-mesons as a function of atomic number was made possible when Steinberger¹ developed an electronic method for detecting π^+ mesons produced by the x-ray beam of the Berkeley synchrotron. McMillan, Peterson, and White² had previously carried on photo-meson studies with nuclear plates, but this method of study would be exceedingly laborious to apply to the study of a large group of elements, although it does have the advantage of allowing the study of π^- mesons as well.

Steinberger and Bishop³ investigated the production of π^+ mesons made by the x-rays of the synchrotron on hydrogen and carbon. They examined meson energies between 35 and 105 Mev and angles between 45° and 135° to the x-ray beam. In addition to obtaining valuable data on the hydrogen cross section, they showed the hydrogen cross section to be very much larger than the cross section per proton in carbon.

Chew and Steinberger⁴ have suggested that exclusion principle arguments similar to those used in their paper discussing the π^-/π^+ ratio of mesons produced in nucleon-nucleon collisions, can also be used to explain the anomaly in the cross section of carbon and hydrogen. The reaction producing a π^+ meson is considered to be



In the case of the production of π^+ mesons from carbon it is felt that only the protons in the nucleus can enter into the primary reaction. For hydrogen all of phase space is available to the recoil neutron, while for carbon the low level neutron states are already occupied. Therefore, at all available energies the cross section per proton in carbon should be much less than that

of hydrogen. Calculations are in progress to obtain more quantitative estimates of this effect.

In order to obtain more information about this effect it was desirable to study the relative cross sections of the lighter elements to see whether the cross sections per proton of the intermediate elements, lithium, beryllium, and boron are close to that of carbon, whether there is a gradual transition from carbon, or whether there are large variations in this cross section in going from one element to another with slightly higher atomic number. It is possible that nuclear shell structure can play an important role in determining the cross section.

At the same time it appeared desirable to evaluate the relative cross sections of the heavier elements. Any anomalies or general relationships derivable from these relative cross sections could also have theoretical significance.

The method of electronic detection developed by Steinberger is a variation of that first used by Rasetti⁵ for the detection of μ mesons in cosmic rays. The method is also very closely related to the technique used by Alvarez⁶ for the detection of π^+ mesons produced by the Berkeley 184-in. cyclotron.

The method of electronic detection used in this experiment and described below was identical to that developed by Dr. Steinberger.

II General Description of Experiment.

The experiment consisted of comparing the π^+ meson yields from various targets placed in the x-ray beam of the synchrotron. The measurement was done on mesons leaving the target at an angle of 90° to the direction of the x-ray beam.

The energy of the electron beam of the synchrotron was approximately 317 Mev in all measurements.

Two meson energy ranges were examined; 42 Mev and 76 Mev with widths of ± 7 Mev and ± 6 Mev respectively. 76 Mev was chosen as the high energy region since in the carbon data previously obtained by Steinberger, the cross section dropped off rather rapidly above that energy, while 42 Mev was chosen since below that energy the background became excessive.

The elements investigated were hydrogen (by subtracting the carbon cross section from the CH_2 cross section) lithium, beryllium, boron, carbon, aluminum, copper, tin, and lead. To investigate more elements or more than two energy ranges would have greatly increased the synchrotron time necessary for the experiment and have given little more pertinent information, especially since it was felt necessary to treat each day's data independently. In each run it was desirable that every element be measured once at both of the meson energies.

III Discussion of the Method.

1. Use of μ^+ Meson Decay for the Detection of the π^+ Meson.

It is known that μ^+ mesons have a mean life of 2.1 microseconds, decaying into a positron (plus probably two neutrinos). Such a decay time can be measured with standard electronic techniques. Since a π^+ meson decays into a μ^+ meson (plus probably one neutrino) it should be possible under some circumstances to detect a π^+ meson by means of the characteristic 2 microsecond decay of its μ^+ meson.

In the experiment under discussion it was desired to detect those π^+ mesons produced by a beam of x-rays passing through targets of various

elements.

If a π^+ meson stops in an anthracene or trans-stilbene crystal, the meson will lose energy in the crystal and thus excite molecular energy states which later emit light. The light can be picked up by a photomultiplier, converted into electronic energy, and amplified. In this energy region the resultant pulse will be of height proportional to the energy lost in the crystal. The light from the crystal and the consequent current in the photomultiplier will have a duration of about 10^{-8} seconds but the pulse from the amplifier will have a duration of approximately 10^{-7} seconds because of the resolving time of the electronic circuits. The π^+ meson will decay into a μ^+ meson in about 10^{-8} seconds. Since the μ^+ meson has an energy of approximately 4 Mev it will in most cases stop in the crystal. The pulse caused by it will not be resolved from the pulse of the incident π^+ meson but will add to its size. With about 2×10^{-6} seconds mean life the μ^+ meson will decay into a positron. The positron will in general not be stopped by the crystal but can lose up to several Mev in it.

The first pulse can be used to trigger a series of gates, the first gate starting for example 0.5 microseconds after the pulse and lasting until 2.5 microseconds, the second starting at 2.5 microseconds and lasting until 4.5 microseconds, etc. If a second pulse occurs at the same time as one of these gates, this fact can be recorded by means of a coincidence circuit, scaler, and register. If in a series of counts a 2.1 microsecond mean life were recorded, this would be evidence that π^+ mesons were being stopped in the crystal. It must however, be proved that there is no other possible cause for such a mean life.

The μ meson which was detected in this process might not have been

produced by the decay of a π^+ meson which stopped in the crystal. However, nuclear plate data (Peterson, White, and Gilbert⁷) show no evidence of μ mesons being produced in a carbon target and set an upper limit for the cross section for this process at 8 percent of the cross section for production of π^+ mesons. Theory predicts a very small cross section and as a result the possibility of an error due to μ mesons from the target has been ignored.

2. Analysis of Error Caused by μ^- and π^+ Mesons Decaying in Flight.

Another source of μ^+ or μ^- mesons is the π^+ or π^- mesons which decay in flight. In this experiment the distance from the target to the crystal was approximately 20 cm. Consider the number which would decay at the two meson energies which were measured. At 76 Mev $\beta = .77$ and at 42 Mev $\beta = .64$. Correcting for the relativistic time dilation:

$$\Delta t = \frac{\Delta t'}{\sqrt{1 - \beta^2}} \quad \Delta t_{76} = 1.5 \Delta t'_{76} \quad \Delta t_{42} = 1.3 \Delta t'_{42}$$

values were obtained for the time of flight:

$$t'_{76} \cong 6 \times 10^{-10} \text{ sec.} \quad t'_{42} \cong 8 \times 10^{-10} \text{ sec.}$$

If a 1.97×10^{-8} second mean life for π^+ mesons is used (Martinelli and Panofsky⁸) the following relationship is obtained:

$$\frac{I_{76}}{I_0} = e^{-\lambda t} = .97$$

$$\frac{I_{42}}{I_0} = .96$$

Therefore at 76 Mev about 3 percent and at 42 Mev about 4 percent of the π^+ mesons decayed in flight. Actually absorbers reduced the average energy so

that about 4 percent of the 76 Mev mesons and 4.5 percent of the 42 Mev mesons decay in flight. There is no reason for assuming a different mean life for a π^- than for a π^+ meson.

A calculation must be made of the percentage of the μ mesons formed in this way which would have reached the crystal. The evaluation of this can be assisted by considering a simplified geometry of a point target and a point crystal. If equal numbers of mesons are leaving the target in all directions, the flux through any part of a sphere surrounding the target will depend only on the number of mesons produced. If some of the π mesons decay into μ mesons before reaching the sphere, the direction of motion of the μ meson being different from that of the π , the number of mesons crossing the surface of the sphere will not be changed. Hence, if a crystal is placed outside the sphere, it will measure the same flux of mesons regardless of the decay of the π mesons and the angular directions of the μ mesons produced thereby. Even if some of the π mesons which are heading toward the crystal decay into μ mesons which go in a different direction and miss the crystal, an equal number of π mesons which are going to miss the crystal will decay into μ mesons which will hit the crystal. Of course the range of the μ mesons produced will be different from that of the π mesons producing them but this effect will be compensated for by μ mesons from other energy ranges.

In the actual geometry used the effect of the collimation must be considered. In order to calculate this effect the difference in angle between the π and μ must be evaluated.

To compute the maximum angle between the direction of the π meson and the μ produced by its decay relativistic equations must be used.

Let \underline{v} be the velocity of the π meson and $\beta = \frac{v}{c}$. Let U_x^0 and U_z^0

be the velocity components of the μ meson in the coordinates of a system in which the π meson is at rest. Let \underline{v} be in the X direction. Then if U_X and U_Z are the velocity components of the μ meson in the laboratory system,

$$U_X = \frac{U_X' + v}{1 + \frac{v}{c^2} U_X'} \quad U_Z = \frac{U_Z' \sqrt{1 - \beta^2}}{1 + \frac{v}{c^2} U_X'}$$

The angle θ between the direction of the π meson and the μ meson will be such that $\text{Tan } \theta = \frac{U_Z}{U_X}$.

$$\text{Tan } \theta = \frac{U_Z' \sqrt{1 - \beta^2}}{U_X' + v}$$

For the maximum angle $U_X' = 0$.

$$\text{Tan } \theta \text{ max} = \frac{\frac{U_Z'}{c} \sqrt{1 - \beta^2}}{\beta}$$

For the 76 Mev case $\beta = 0.77$ and $\frac{U_Z'}{c} = 0.27$. $\text{Tan } \theta \text{ max} = 0.23$.

For the 42 Mev case $\beta = 0.64$ and $\frac{U_Z'}{c} = 0.27$. $\text{Tan } \theta \text{ max} = 0.32$.

The collimator reduces the number of μ mesons which reach the crystal only if it interferes with π mesons which would send a μ meson into the crystal when they decay in flight. Since the angle between the π meson and its μ is relatively small, the actual collimator used in this experiment should have reduced the number of μ mesons hitting the crystal by about 20 percent. As a result about 3-1/2 percent of the 42 Mev π mesons and about 3-1/4 percent of the 76 Mev π mesons decayed into μ mesons which would reach the crystal. In the case of the π^+ mesons this means that almost all π^+ mesons were counted regardless of whether or not they decayed in flight. Therefore, no error was introduced in this experiment by the π^+ mesons which

decayed in flight since only relative cross sections were measured. However about 3-1/2 percent of the π^- mesons decayed into μ^- mesons which were counted. From the data of Peterson, White, and Gilbert⁷ the ratio of π^-/π^+ photo-mesons from carbon is about 1.3. If the ratio stays approximately constant for various elements, the μ^- mesons which reached the crystal introduced negligible error. In the case of hydrogen, however, no π^- mesons have been observed by Cook⁹ in his nuclear plate work. Therefore it appears that the hydrogen cross section should be increased about 4-1/2 percent before comparing it with other cross sections. It is unlikely that the π^-/π^+ ratio will fluctuate greatly in the case of the other elements measured and as a result it is improbable that any other correction should be made.

3. Other Possible Causes of a 2 Microsecond Mean Life.

Many of the π mesons would stop in nearby materials. The π^- mesons would produce stars and hence cause no delayed coincidence in the crystal. The energy of the μ^+ meson from a decaying π^+ is about 4 Mev and hence only a few near the edge could enter the crystal. The circuit bias was such that these would not be counted although no error would be introduced if they were. No delayed coincidence could be introduced by the π^- mesons which stopped in the crystal. In the meson studies performed by Bradner¹⁰ and the Berkeley film group an upper limit has been set on the percentage of π^- mesons which decay into μ^- mesons after stopping in a nuclear plate. This number is less than 0.1 percent of the π^- mesons. Even these can probably be accounted for as due to other effects.

There is the possibility of having produced an induced radioactivity with the same half-life as the μ^+ decay. A particle which produced a pulse on entering the crystal could also have produced a nuclear transformation

resulting in a 2 microsecond mean life. Since the crystals are composed of hydrogen and carbon, it must be a radioactive element produced in some way from these elements. No such activity is known. Moreover, the delayed counts disappeared when the peak energy of the synchrotron dropped below the threshold energy for meson production.

If a 2 microsecond activity was detected, it therefore should have been due primarily to π^+ mesons with about 4-1/2 percent of the counting rate being caused by the π^- mesons. The π^- mesons cause an error of 4-1/2 percent in the cross sections only if the π^-/π^+ ratio varies more than a factor of 2 in the various elements measured or if the $\pi^- - \mu^-$ mean life is much shorter than the $\pi^+ - \mu^+$ mean life obtained by Martinelli and Panofsky.

IV Experimental Details.

1. Methods for Reducing Background.

The actual problem of counting mesons was complicated by a large background of accidental counts due to other ionizing radiations from the target, from the x-ray beam and from the synchrotron itself.

A large part of the background could be eliminated by shielding the crystal with lead. At least 6 in. of lead was placed on all sides of the crystal except for a channel to the target. See Fig. 1 and 2. This channel acted as a collimator and gave an angular resolution of ± 8 degrees. In this channel aluminum absorbers were placed to select the correct energy range of meson.

To explain how the background was further reduced requires a description of some details of synchrotron operation. It is assumed that the reader understands the general principles of the synchrotron.

During the time that the electron beam is accelerated the magnetic

field at the orbit varies in time as shown in Fig. 3. Since during most of the time the electrons are travelling at nearly the velocity of light the energy of an electron varies linearly with the magnetic field. Electrons are injected at time a and accelerated by betatron operation until time b. At this time the flux bars saturate and the oscillator is turned on. The acceleration is continued until time c, the oscillator is turned off, and the orbit of the beam contracts until the beam hits the target. X-rays are emitted from the target in a very narrow forward cone. The total time during which the beam of x-rays exists is 10 microseconds per cycle of operation. This cycle is repeated 6 times a second. It is this beam of x-rays which was used to produce the mesons. Since the x-ray beam exists only 60 microseconds per second the accidental rate in a coincidence circuit should be very high. If N_1 and N_2 are the numbers of counts in the two channels put in coincidence, T is the resolving time (total time during which coincidence can occur), and "duty cycle" means the ratio of the time the x-ray beam exists to the total time, the number of accidental coincidence counts in an interval of time are given by the following formula:

$$\text{Accidental counts} = \frac{N_1 N_2 T}{\text{Time} \times \text{Duty Cycle}} .$$

In another type of synchrotron operation, the electron beam can be made to collapse into the target in about 2000 microseconds by turning the oscillator off slowly. It can be seen that this will increase the duty cycle and therefore reduce the accidental coincidence rate by a factor of 200.

2. X-ray Spectrum.

Since the beam was spread out in time, the energy of the electrons hitting the target was spread out to some extent. As the beam of x-rays

came out at a time corresponding to the top of the sine wave of magnetic field, the energy of the electrons causing the x-rays did not change very rapidly with time. The change of intensity of the x-ray beam with time could be studied by placing a scintillation counter in the beam, and putting the output on an oscilloscope. Fig. 3 shows the usual plot of intensity vs. time which was obtained. The shape of this intensity distribution changed very little.

The timing of the beam with respect to the peak magnetic field could be continuously monitored by placing the beam picture and a pip occurring at the peak magnetic field on the same oscilloscope sweep. The peak of the beam intensity occurred approximately 1200 microseconds before the peak magnetic field, with a maximum variation of about 200 microseconds. The actual peak magnetic field was such that the corresponding electron energy was about 326 Mev. The real peak energy was not known to better than ± 10 Mev due to a drift of synchrotron energy. This beam was spread approximately 30 Mev in the type of operation used.

The x-rays produced by the synchrotron beam should have an energy distribution much like the theoretical Bremstrahlung spectrum. Modifications must be made because of the energy loss of the generating electrons in the synchrotron target, the scattering and intensity loss of x-rays in this target, and the effect of the collimator used. These theoretical corrections have been made by Mr. Christian and the curves are shown in Fig. 4. In addition the spectrum is affected by the spread in the beam energy. The calculation of this effect has been made by Mr. Bishop. The resultant curve is shown in Fig. 4. This is a representation of the x-ray beam intensity at any one time. However, the peak energy was not known to closer than ± 10 Mev and varied an additional ± 10 Mev.

3. Integration of X-ray Beam.

Two ionization chambers were used for measuring the x-ray intensity, one was placed in the x-ray beam behind the experimental target and the other in front of the target. The instantaneous output of the chamber behind the target was used to drive a watt-hour meter which thereby recorded a number proportional to the total number of x-ray quanta which passed through it. This integrator was slightly non-linear (about 15 percent over a factor of 3 in beam intensity) and hence was useful only when the intensity of the x-ray beam was constant. The chamber in front of the target was so operated that the current from it charged a condenser which was discharged at a predetermined voltage, thereby actuating a register. The linearity and stability of this instrument were good to 5 percent. Both of the beam integrators were used simultaneously and the readings compared to be sure no violent fluctuations were taking place. The reading of the chamber in front of the experimental target was used in all data except in one run which was made at approximately constant beam intensity. Since this experiment was concerned only with relative cross sections, no absolute reading of the integrator was necessary.

4. Detection Equipment.

Measurements were made by placing the target of the element to be investigated in the x-ray beam and placing the crystal used for detecting the mesons at about 20 cm distance and at an angle of 90° to the beam direction. At least 6 inches of lead were placed on all sides of the crystal except for a channel to the target.

In order to reduce the background a coincidence telescope was made by placing another crystal between this crystal and the target. Gate circuits were triggered only if a coincidence of pulses from these two crystals occurred. In addition a third crystal was placed behind the counting crystal

in anti-coincidence with the first two crystals. The gate circuits were triggered only if a particle entered the first two crystals and not the third, thereby probably stopping in the 2nd crystal. The first crystal pulse amplification was such that all particles losing over about 6 Mev in it were counted, the third crystal such that all losing over about 1 Mev were counted, while the output of the 2nd crystal amplifier was divided into two channels: IIA such that pulses of over 8 Mev and IIB such that pulses of over 2 Mev were counted.

Thus the pulse of a heavily ionizing particle occurring at the same time in I and IIA and no pulse in III were required to trigger the gate circuits, while the pulse of even a weakly ionizing particle could be counted in IIB and in coincidence with the gates.

A block diagram of the electronics is given in Fig. 5. In Fig. 6 signals are shown which are characteristic of those which would occur at various parts of the circuit if a meson were counted. (Points are labeled in the block diagram.) Fig. 7 is a photograph of the electron equipment used.

The crystals used were of anthracene and trans-stilbene approximately 3/4 in. thick and 2 in. x 2 in.

5. Background Measurement.

In operation there was a fairly high accidental counting rate. This could be computed by using the single counting rate for channel IIB, the number of times the gates were triggered, the resolving time, the duty cycle, and the time required for the run. Measurement of the duty cycle must be done experimentally so in practise it was better to make an experimental estimate of the background for each run. This was done by triggering a gate from a fraction of the pulses in channel III (the single counting rate of this channel was too high to use for this purpose). These gates were put in

coincidence with the output of IIB. The accidental rate in one of the meson gates would be given by the following relationship:

$$\text{Background} = \frac{\text{Meson Gate Width} \times \text{Number of Meson Gates} \times \text{Counts in Background Gate}}{\text{Background Gate Width} \times \text{Number of Background Gates}}$$

The ratio of the effective gate widths could be measured experimentally using a gamma-ray source. Pulses from one of the crystals were used to trigger all of the gates and pulses from another crystal (or the same crystal) could be put in coincidence with the gates. The number of pulses recorded should be proportional to the ratio of the gate widths.

The background obtained in this manner was subtracted from the counts registered as passing through each of the gates. The remaining counts should have been due to mesons decaying. That this was actually the case was confirmed by the fact that the data so obtained gave a mean life for μ electron decay which was 2.1 microseconds, within the error of the statistics and calibration.

6. Stability of the Electronic Equipment.

To evaluate the accuracy of the data taken, the stability of the electronics and the effect of any instability on the meson counting rate must be known. For this purpose the variation of the meson counting rate with the gain of the amplifiers and photomultipliers in the three channels has been studied. The meson counting rate was virtually independent of whether channel III was used. It can be seen in Figs. 8, 9 and 10 that plateaus existed for meson counting rate versus gain in channels I and IIA. The single counting rates on the other hand increased rapidly as the gain was increased. Since the single counting rate of each of these channels was measured, it could be used as a criterion of whether the gain had changed sufficiently to cause appreciable inaccuracy. Channel IIB had only a very slight plateau and as a

result this channel had to be carefully monitored.

To insure that the gain of this channel was correct a gamma-ray standard was periodically placed at a fixed distance from the crystals and the gain of channel IIB set so as to obtain a predetermined counting rate. Channel III was also monitored in this way but there was insufficient energy in the gamma-rays for them to be recorded in channel I or IIA. As a result one of the targets was used as a standard. The single counting rates of all of the channels were measured with this target, then two other targets were run, and then this standard run again. The criteria for acceptable bracketed runs were that channels I, IIA, and III should not vary more than 30 percent and IIB more than 10 percent. A part of this percentage would be statistical error.

Each day's data were evaluated separately. Therefore an advantage was gained by running all targets at least once each day at both of the two energies measured. An attempt was made to do this for all targets except tin and lead which required running at such a low beam intensity and therefore for such long periods as to make it impossible to run all of the other targets on the same day.

7. Design of Targets.

In order to avoid the calculation of geometric effects all targets were made as closely as possible the same physical shape. See Fig. 11. The size and shape were determined by the following considerations: The target area was made larger than the beam area so that the target would not have to be located accurately in the direction at 90° to the beam. A 1 in. collimator was used for the beam and the distance of the target from the collimator was such that the beam had a diameter of approximately 1-1/2 inches. The targets were all 2 in. high and at least 2-1/2 in. wide. The target

thickness in the direction of the x-ray beam was made small. This made it possible to correct for the attenuation of the beam without introducing appreciable error. Targets were so designed that mesons of the energy investigated could lose approximately equal energies in all targets (except tin and lead). This problem was simplified by taking the targets thin in the direction (90° to the x-ray beam) in which mesons were to be counted. As a result the targets were all of approximately $1\frac{1}{2}$ grams/cm².

The lightest element measured was a compressible boron powder. The next was solid lithium. The boron powder was held in the correct shape by a thin aluminum container. A similar container was necessary for the lithium to protect it from the air. A duplicate empty container was measured and its counting rate subtracted from the lithium and boron rates. No containers were necessary for the other target materials. With the exception of tin, lead, and copper the other target thicknesses were made to correspond in meson energy loss to the lithium target. The boron powder could be compressed to make it approximately the equivalent. The other targets were made in several layers. The layers were mounted at a 45° angle to both the x-ray beam direction and the direction of the crystals. Thus they presented a low average density to the x-ray beam and the correct average density to the mesons.

It was found that the counting rate for mesons doubles in going from 42 Mev to 76 Mev meson energy. Since the targets were approximately $4\frac{1}{2}$ Mev thick or $2\frac{1}{4}$ Mev thick for the average mesons, little error was introduced by making the targets too thin or too thick. Therefore in the case of lead and tin it was easier to correct for the meson range than to correct for the attenuation of the x-ray beam. As a result targets about $1/7$ and $1/10$ as

thick were used for these two elements.

Corrections were made for both the attenuation of the x-ray beam and differences of meson range in the targets.

Beryllium and boron were the only elements tested which had an appreciable amount of impurity. Analysis showed 1 percent impurity in the beryllium, primarily Al, Ca, and Mg. There was a 4 percent impurity in the boron, primarily Mg.

The dependence of the cross section on the atomic number shows that any impurity of a heavier element should decrease the cross section slightly. The beryllium impurity required less than 0.1 percent correction and was neglected. The boron impurity required a correction of +0.9 percent at 76 Mev and +0.7 percent at 42 Mev.

8. Scattering of Mesons in the Absorber.

Scattering took place in the absorbers which determined the energy range measured. For coulomb scattering however, the geometry was such that approximately the same number scattered in as scattered out. Since relative cross sections were measured, only the difference in the coulomb scattering at the two energy ranges was effective in causing an error. This error was estimated at less than 1 percent and has been neglected.

The nuclear absorption and scattering cross sections are not well enough known to make a correction possible. If the cross sections are equal to the nuclear area approximately a 25 percent correction would be required at 76 Mev and an 8 percent correction at 42 Mev, or since only relative cross sections were measured the cross sections at 76 Mev would be 17 percent too low.

9. Computations of Energies and Relative Cross Sections.

All measurements were made at the same energy of the x-ray beam and at two meson energies. The meson energies were those with the two ranges: 1/2 in. of aluminum + crystal I + range to stopping point in crystal II and 2-1/2 inches of aluminum + crystal I + range to stopping point in Crystal II. The crystals were of trans-stilbene and anthracene 0.740 in. and 0.835 in. thick, and 2 in. by 2 in. in area.

For all elements except aluminum, the meson energies were computed using the Proton Range Energy data calculated by Aron, Hoffman, and Williams¹¹. For aluminum, J. H. Smith's¹² tables were used. The proton range energy computations were applied to mesons by using the following relationships:

$$\frac{dE}{dX} \text{ meson} = \frac{dE}{dX} \text{ proton} \left(E_{\text{proton}} = E_{\text{meson}} \times \frac{\text{proton mass}}{\text{meson mass}} \right)$$

and

$$\text{Range} \left(E_{\text{meson}} \right)_{\text{meson}} = \frac{\text{meson mass}}{\text{proton mass}} \times \text{Range} \left(E_{\text{proton}} = E_{\text{meson}} \times \frac{\text{Proton mass}}{\text{Meson mass}} \right)$$

A meson mass of 276 electron masses was used in all computations. The resultant energies were 42 ± 7 Mev and 76 ± 6 Mev.

The relative cross sections were computed as follows:

$$\sigma = \frac{\text{Number of counts}}{\text{Integrated x-ray beam}} (N) \times \frac{1}{\text{Width of meson energy range} (R)}$$

$$\times \frac{1}{\text{Number of nuclei per cm}^2 \times \text{solid angle}}$$

Since the geometry remained constant the solid angle could be considered a constant. The number of nuclei per $\text{cm}^2 = \text{Constant} \times \frac{\text{Grams per cm}^2 (W)}{\text{Atomic wt} (A)}$.

If all constant factors are included in a constant K the following formula is obtained for the relative cross section:

$$\sigma = \frac{K N A}{R W}$$

The width of meson energy range (R) counted was different at 42 and 76 Mev. R is 1.33 times larger at 42 Mev than at 76 Mev. If the relative cross sections at the two energies are to be compared the 76 Mev cross section must be increased by a factor of 1.33.

V Results of Experiment.

1. Data of Typical Graphite Run.

The type of data recorded in measuring the meson yields can be best illustrated by giving the actual data recorded in one of the many runs with graphite. This run was made with a 2-1/2 in. aluminum absorber in place.

Integrator 1	5
Integrator 2	73
Time	7.2 minutes

Numbers of Single Counts

Crystal I	21.1 x 256
Crystal IIA	13.0 x 256
Crystal IIB	36.3 x 256
Fraction of Crystal III output	29.5 x 256

Coincidence Counts

Crystals I and IIA anticoincidence with III	3.9 x 256
IIB and Background Gate	20
IIB and Meson Gate 1	21
IIB and Meson Gate 2	6
IIB and Meson Gate 3	6
IIB and Meson Gate 4	3

Calculated Counts

Background Counts in Each Gate	2.48
Mesons Recorded in Gates 1 and 2	22

2. Summary of the Data.

Seven runs were made to obtain the data. The data obtained in each run were analyzed separately. Since only relative cross sections were obtained, any changes taking place in the electronic equipment between runs could not introduce inaccuracy.

The data were combined weighting the measurements according to the inverse squares of the proportional standard deviations.

If R_1, R_2, R_3, \dots are the data and E_1, E_2, E_3, \dots the proportional standard deviations, the resultant datum is

$$R = \frac{\frac{R_1}{E_1^2} + \frac{R_2}{E_2^2} + \frac{R_3}{E_3^2} + \dots}{\frac{1}{E_1^2} + \frac{1}{E_2^2} + \frac{1}{E_3^2} + \dots}$$

The new proportional standard deviation becomes

$$E = \sqrt{\frac{1}{\frac{1}{E_1^2} + \frac{1}{E_2^2} + \frac{1}{E_3^2} + \dots}}$$

The resultant data are given on the following two pages as a number proportional to the number of meson counts per unit beam such that the sum is approximately one.

2-1/2 inches of aluminum absorber

Target Material	Counts per Unit Beam	Percent Standard Deviation
CH ₂ (polyethylene)	0.0703	5.6
C (Graphite)	0.0491	4.7
Li	0.0744	7.7
Be	0.0525	9.3
B	0.0530	9.0
Al	0.0507	9.0
Cu	0.0288	14.5
Sn	0.00410	36.2
Pb	0.00408	44.0
Empty Aluminum Container	0.00075	100.
No target	0.00094	100.

1/2 inch aluminum absorber

Target Material	Counts per Unit Beam	Percent Standard Deviation
CH ₂ (polyethylene)	0.0972	6.8
C	0.0870	5.8
Li	0.1187	9.8
Be	0.0919	11.1
B	0.0946	10.2
Al	0.0989	11.0
Cu	0.0613	18.2
Sn	0.0134	23.3
Pb	0.00313	66.4
Empty aluminum container	0.00283	46.5
No target	0.00073	94.

Targets Used:	Weight Grams	Width (Height = 2")	Grams/cm ²
CH ₂ (polyethylene)	48.20	3.50"	1.08
C (graphite)	67.24	3.50"	1.49
Lithium	58.2	2.50"	1.80
Beryllium	78.4	3.75"	1.62
Boron	47.55	2.50"	1.47
Aluminum	83.85	3.50"	1.86
Copper	71.09	3.50"	1.57
Tin	30.3	6.00"	0.391
Lead	16.4	5.00"	0.254

The empty aluminum container rate is subtracted from the lithium and boron data, while the no target rate is subtracted from the data of the other elements. A relative value for the uncorrected cross sections is then found by the following relationship:

$$\sigma = \frac{K N A}{R W}$$

Element	Cross Section	Percent Standard Deviation
2-1/2 inches of aluminum absorber		
CH ₂	20.2 K	6
C	8.61 K	5
Li	6.26 K	11
Be	6.36 K	10
B	8.48 K	15
Al	16.0 K	9
Cu	24.9 K	15
Sn	21.5 K	55
Pb	56.0 K	65
1/2 inch of aluminum absorber		
CH ₂	28.1 K ^o	7
C	15.4 K ^o	6
Li	9.86 K ^o	10
Be	11.2 K ^o	11
B	14.9 K ^o	11
Al	31.6 K ^o	11
Cu	54.2 K ^o	19
Sn	85.3 K ^o	25
Pb	43.3 K ^o	91

3. Corrections.

The following corrections must be applied to the cross sections:

The hydrogen cross section must be increased by 4-1/2 percent since in this data no π^- mesons are included while in the data of the other elements the counts due to μ^- mesons from π^- mesons which decay in flight are included.

Corrections must be made for the attenuation of the x-ray beam in the target. This correction factor takes into account pair production, triplet production, and Compton scattering. The data used were obtained from Heitler's book¹³. The attenuation used is that of the high energy components of the x-ray beam. The correction factor used is 1/2 of the attenuation.

The percent corrections are tabulated below:

CH ₂	+ 0.9 %
C	+ 1.3 %
Li	+ 0.9 %
Be	+ 1.0 %
B	+ 1.1 %
Al	+ 2.7 %
Cu	+ 3.9 %
Sn	+ 1.6 %
Pb	+ 1.6 %

An additional correction must be made since the targets were not all equally thick for meson energy loss. This correction is made by assuming a linear change of counting rate between the 76 and 42 Mev energies. The aluminum target is used as a standard in these computations since it also served in the calculation of energies from the ranges in absorbers and

target. This method of calculation should introduce no appreciable error since in all cases except tin and lead the correction is less than 2 percent. In the case of tin and lead the correction is much less than the standard deviation of the cross section.

The corrections for target thickness are tabulated below:

Target Material	42 Mev	76 Mev
CH ₂	-0.41 %	-0.6 %
C	+0.3	-0.3
Li	+0.2	+0.1
Be	-0.2	-0.4
B	-0.5	-0.7
Al	0.00	0.00
Cu	-1.0	-1.2
Sn	-4.5	-12.1
Pb	-5.1	-13.2

The corrections for the magnesium impurity in the boron are +0.9 percent at 76 Mev and +0.7 percent at 42 Mev.

The total correction which must be applied to each of the cross sections is tabulated on the following page.

Target Material	Percent Correction	
	42 Mev	76 Mev
CH ₂	+ 0.5	+ 0.3
C	+ 1.6	+ 1.0
Li	+ 1.1	+ 1.0
Be	+ 0.8	+ 0.6
B	+ 1.3	+ 1.3
Al	+ 2.7	+ 2.7
Cu	+ 2.9	+ 2.7
Sn	- 2.9	-10.5
Pb	- 3.5	-11.6

In addition a + 4.5 percent correction must be applied to the hydrogen cross section when this is derived.

In the cross section data given above, the cross sections at 42 and 76 Mev are not in terms of the same energy range. This correction is made by multiplying the relative cross sections at 76 Mev by 1.33.

4. Relative Cross Sections.

In the table given on the following page, all corrections have been made and the hydrogen cross section evaluated by subtracting the carbon cross section from the CH₂ cross section. The units are arbitrary.

Meson Energy		76 ± 6 Mev	
Target Element	Relative Cross Section	Standard Deviation (percent)	
CH ₂	27.0	6	
C	11.57	5	
H	8.07	11	
Li	8.41	11	
Be	8.51	10	
B	11.41	15	
Al	21.85	9	
Cu	34.01	15	
Sn	25.59	55	
Pb	65.84	65	
Meson Energy		42 ± 7 Mev	
CH ₂	28.2	7	
C	15.6	6	
H	6.6	17	
Li	9.97	10	
Be	11.29	11	
B	15.09	11	
Al	32.45	11	
Cu	55.77	19	
Sn	82.83	25	
Pb	41.78	91	

The standard deviations given apply between all cross sections except hydrogen and either the C or CH₂ of the same energy region. In this case the hydrogen cross section is dependent on the other two cross sections. As a result the ratio

of the hydrogen and carbon cross sections would have a slightly larger standard deviation than would be computed from the deviations given.

$$\text{At 76 Mev } \frac{\sigma_H}{\sigma_c} = 0.697 \pm 14 \text{ percent}$$

$$\text{At 42 Mev } \frac{\sigma_H}{\sigma_c} = 0.423 \pm 21 \text{ percent}$$

Since it is considered that π^+ mesons are produced by an interaction of the x-rays with the protons in the nucleus it is interesting to tabulate the cross sections in terms of the cross section per proton or $\frac{\sigma}{Z}$

Element	$\frac{\sigma}{Z}$	Percent Standard Deviation
76 Mev		
H	8.07	11
Li	2.80	11
Be	2.13	10
B	2.28	15
C	1.93	5
Al	1.68	9
Cu	1.17	15
Sn	0.51	55
Pb	0.80	65

42 Mev		
Element	$\frac{\sigma}{Z}$	Percent Standard Deviation
H	6.6	17
Li	3.32	10
Be	2.82	11
B	3.02	11
C	2.60	6
Al	2.50	11
Cu	1.92	19
Sn	1.66	25
Pb	0.51	91

These cross sections are plotted against Atomic Number in Fig. 12.

5. Estimate of Error.

Ignoring possible errors caused by nuclear scattering and nuclear absorption of the mesons in the absorption, the sources of error other than those inherent in the statistics of the measurements were: measurement of the target thickness, differences in effective target shape, differences in the location of the targets, shifts in synchrotron energy, measurement of x-ray beam, and changes in the sensitivity of the electronics.

The measurement of the x-ray beam and the instability of the electronics were the primary sources of error. Each could cause an error of about 5 percent in a run. Since the measurements were made at least three times for all elements except tin and lead it is improbable that the maximum possible error occurred.

It seems highly improbable that errors of greater than 7 percent could have occurred in the measurements of Li, Be, B, C, Al, and Cu. Tin and lead could possibly be in error by 10 percent. Since a subtraction method was

used for obtaining the hydrogen cross section, the nonstatistical error in this measurement would normally be larger than the error in the other elements. However, the carbon and CH_2 data used to obtain the hydrogen cross section were obtained in 8 runs for the 76 Mev data and 6 runs for the 43 Mev data. For this reason an estimate of maximum error of approximately 10 percent is made for hydrogen.

The above are estimates of maximum error in addition to the statistical error which is tabulated in terms of the standard deviation.

VI Discussion of Results.

Meson theories do not make any very firm predictions concerning the relative cross sections which should be obtained in the above experiment. However, certain tentative qualitative conclusions can be derived from the data.

Chew and Steinberger have suggested that the large difference between the cross section of hydrogen and the cross section per proton in carbon may be explained by the operation of the exclusion principle on the resultant recoil neutron. The fact that the cross section per proton of lithium, beryllium, and boron are very close to that of carbon lends at least qualitative support to this explanation. The lithium, beryllium, and boron nuclei should not differ much from the carbon nucleus in the availability of unoccupied neutron states. However, it is possible that some other binding energy dependent effect could cause the same type of variation.

Except for the large difference in cross section between hydrogen and the other elements, no large changes in $\frac{\sigma}{Z}$ can be seen which do not fit a smooth curve. Although such a variation was looked for between lithium, beryllium, boron, and carbon, any variation which may exist is obscured by

the statistics.

The other information obtained is that the cross section per proton decreases gradually as Z increases. This decrease is about the same for 42 and 76 Mev mesons.

It is improbable that this decrease can be due to the screening of protons located in the center of the nucleus by competing reactions taking place in the external nucleons. Silverman's work on photo-protons¹⁴ from Cu showed a total cross section for production of protons with greater than 35 Mev energy of approximately $4 \times 10^{-27} \text{ cm}^2$. If this cross section were increased by a factor of 5 because of other possible reactions, a cross section of $2 \times 10^{-26} \text{ cm}^2$ would be obtained. A cross section more nearly equal to the nuclear area would be required before such screening could play an important role.

A different type of screening could be caused by pair production. If the pair production cross section were so large in the immediate region of the nucleus that x-rays were converted into pairs before they could interact with the nucleons, such a Z dependent cross section might be caused. An order of magnitude calculation shows that such an effect can be ignored.

The x-ray photon cannot be localized in a direction transverse to its line of motion to closer than the Compton wavelength, λ_c , of an electron with which it interacts. The cross section can therefore be considered somewhat constant over an area $\pi \lambda_c^2 = 4.7 \times 10^{-21} \text{ cm}^2$, but the pair production cross section for lead at 300 Mev is approximately $42 \times 10^{-24} \text{ cm}^2$. The ratio is 110/1. Thus the chance of a pair occurring as an x-ray passes near a nucleus is of the order of 1 in 100. Little screening can result from this.

Since the energy of the mesons is well above that of the Coulomb

barrier of even lead, it is improbable that the large decrease in cross section between carbon and lead can be accounted for by any Coulomb effect.

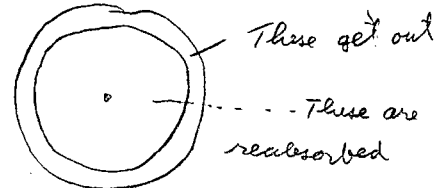
The fact that the cross section for the 76 Mev mesons decreases approximately the same percentage as the cross section for the 44 Mev mesons makes a Coulomb barrier effect even more improbable.

A possible explanation of such a decrease is that it is caused by the interaction of the mesons with nucleons. This might prevent the mesons produced in the interior of the nucleus from escaping. If the mesons have a mean free path in nuclear matter which is short compared to the nuclear radius, this would cause the cross section per proton to decrease as

$$\frac{\text{Surface Area of Nucleus}}{\text{Volume of Nucleus}}$$

or since the surface area is proportional to $A^{2/3}$

$$\frac{\sigma}{Z} \propto \frac{A^{2/3}}{A} = \frac{1}{A^{1/3}}$$



Dr. Chew¹⁵ suggests that an additional cause of such a surface effect could be that there is more phase space available to the recoil neutron when a π^+ meson is produced from a proton near the surface of the nucleus than when the meson is produced from a proton in the interior of the nucleus.

In Fig. 13 $\frac{1}{A^{1/3}}$ curves have been superimposed on the observed data. These curves are normalized to the data at carbon. It can be seen that the fit is quite good. Although this does mean that it is possible for the observed decrease in $\frac{\sigma(z)}{Z}$ to be explained by some type of surface effect, the probable errors are such that a great many types of curves could be made to fit the data.

There is no valid reason for assuming that the observed decrease is

caused by a surface effect.

VII Acknowledgements.

I wish to express my gratitude to Dr. J. Steinberger for his assistance in all parts of this work and to Professors E. M. McMillan and W. K. H. Panofsky for their interest and advice. Professors G. Chew and R. Serber and Mr. Brueckner were of great assistance in their discussions of the theoretical implications. Messrs. Conway and Moore helped greatly in their analysis of the purity of the beryllium and boron. My sincere thanks also go to Mr. Walter Gibbins and the entire synchrotron crew.

This work was sponsored by the Atomic Energy Commission.

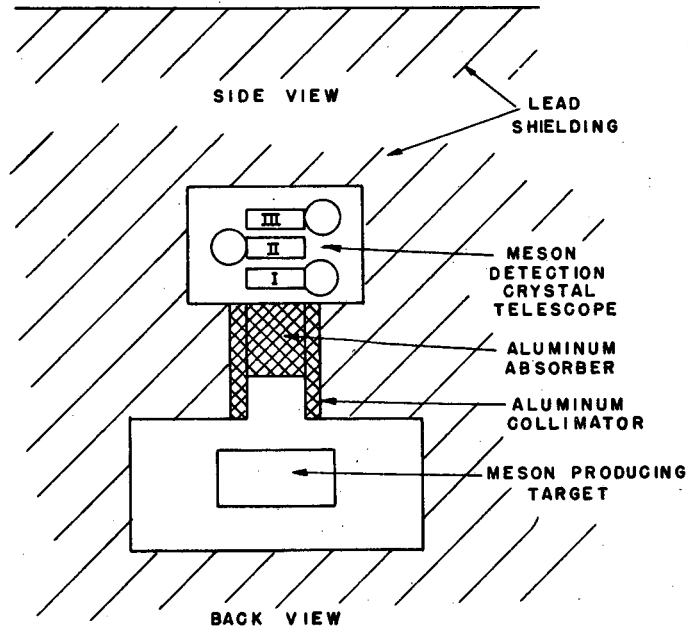
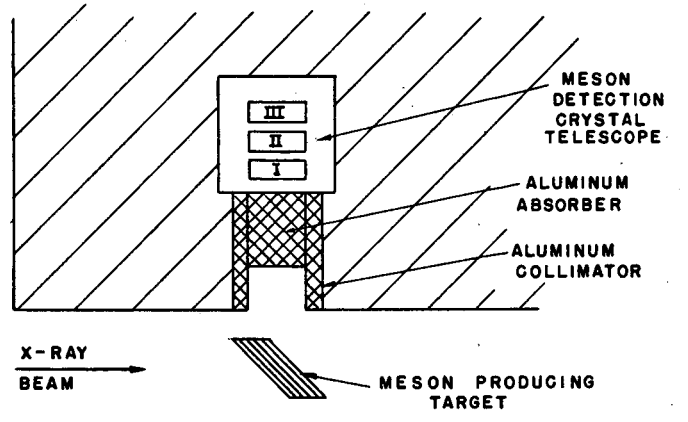
References

1. J. L. Steinberger and A. S. Bishop, Phys. Rev. 78, 319, (1950) and UCRL-631.
2. E. M. McMillan, J. M. Peterson, and R. S. White, Science 110, 579
3. J. L. Steinberger and A. S. Bishop, UCRL-632
4. G. F. Chew and J. L. Steinberger, To be published Phys. Rev. 78, No.4 (1950)
5. F. Rasetti, Phys. Rev., 60, 198 (1941).
6. L. W. Alvarez, A. Longacre, V. C. Ogren, R. E. Thomas, Phys. Rev. 77, 752 (1950).
7. J. M. Peterson, R. S. White, and W. S. Gilbert, Private Communication.
8. E. Martinelli and W. K. H. Panofsky, Phys. Rev. 77, 465 (1950).
9. L. Cook, Private Communication.
10. H. Bradner, Review of Work on Artificially Produced Mesons; UCRL-486,6.13.
11. W. A. Aron, B. G. Hoffman, and F. C. Williams, Range Energy Curves, UCRL-121.
12. J. H. Smith, Phys. Rev. 71, 32 (1947).
13. W. Heitler, The Quantum Theory of Radiation, Oxford University Press, 1944.
14. A. Silverman, Private Communication.
15. G. F. Chew, Private Communication.



FIG. 1

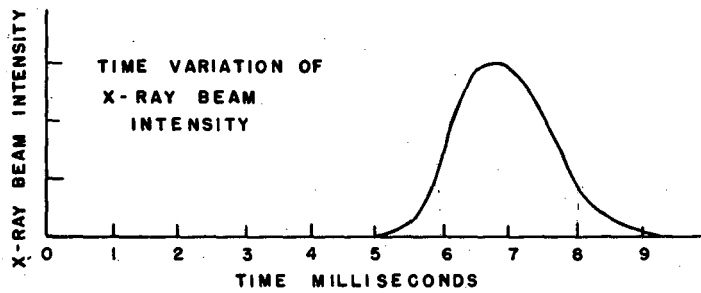
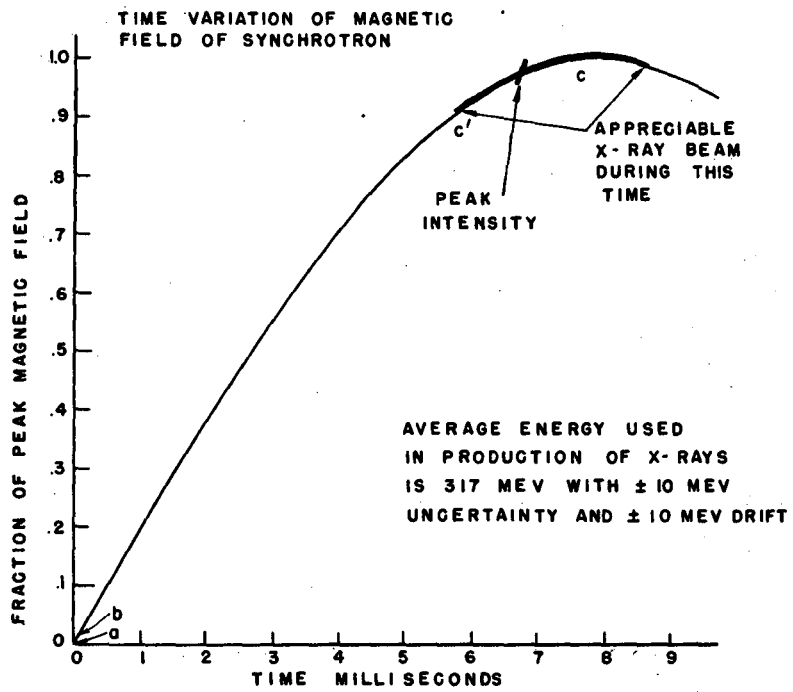
SYNCHROTRON AND SHIELDING FOR MESON DETECTION
TELESCOPE.



ARRANGEMENT OF TARGET, ABSORBERS, AND MESON DETECTION TELESCOPE

FIG. 2

MU 246



MU 247

FIG. 3

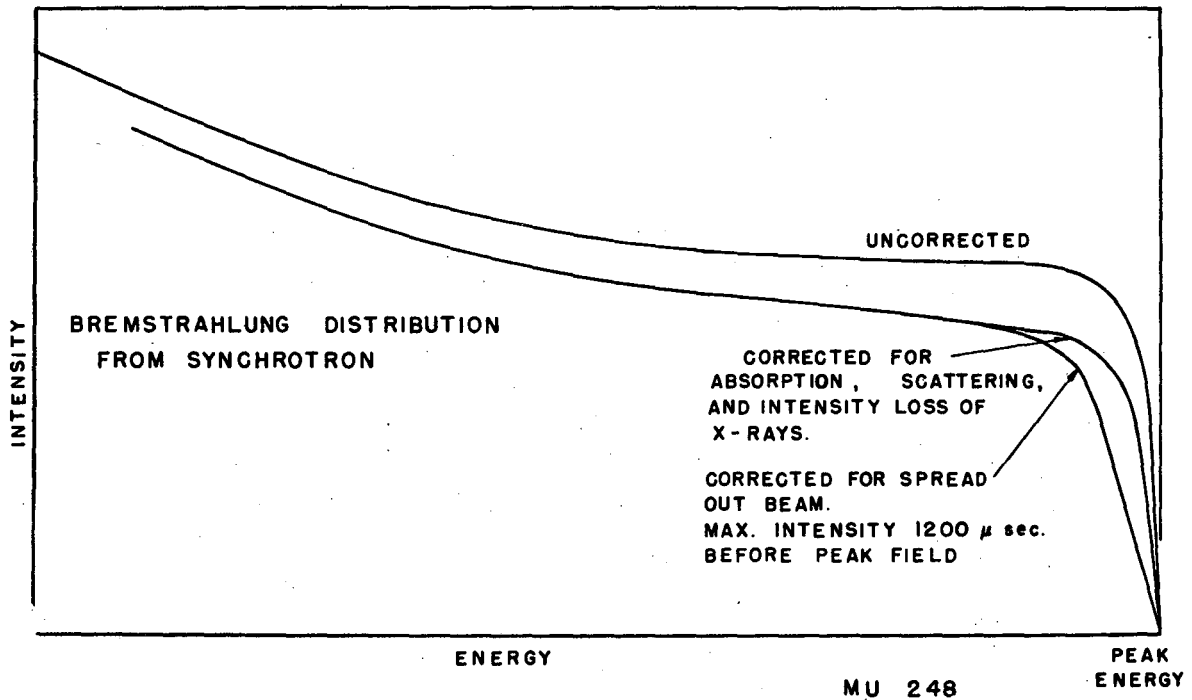
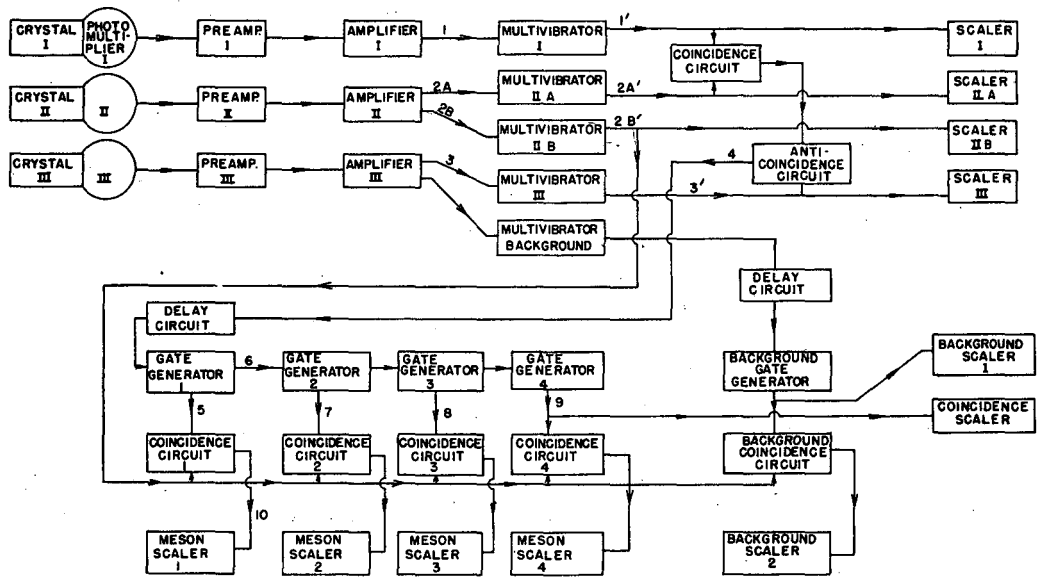


FIG. 4



MU 249

BLOCK DIAGRAM OF ELECTRONICS
FIG. 5

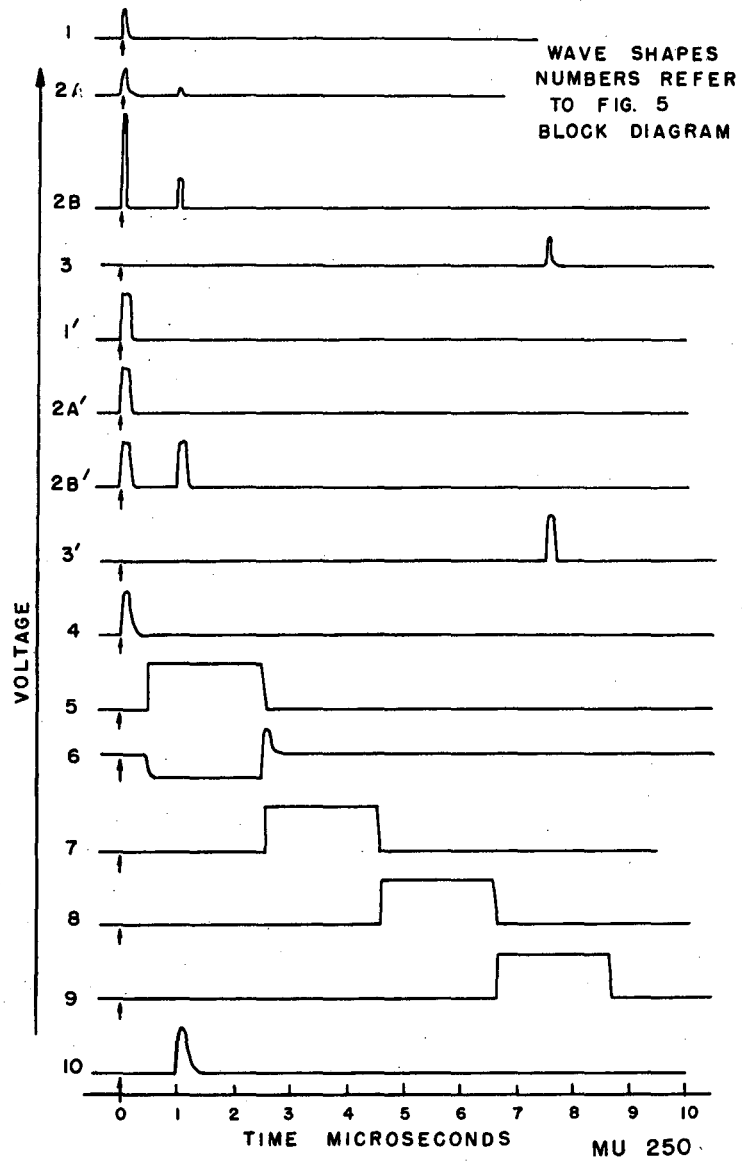


FIG. 6

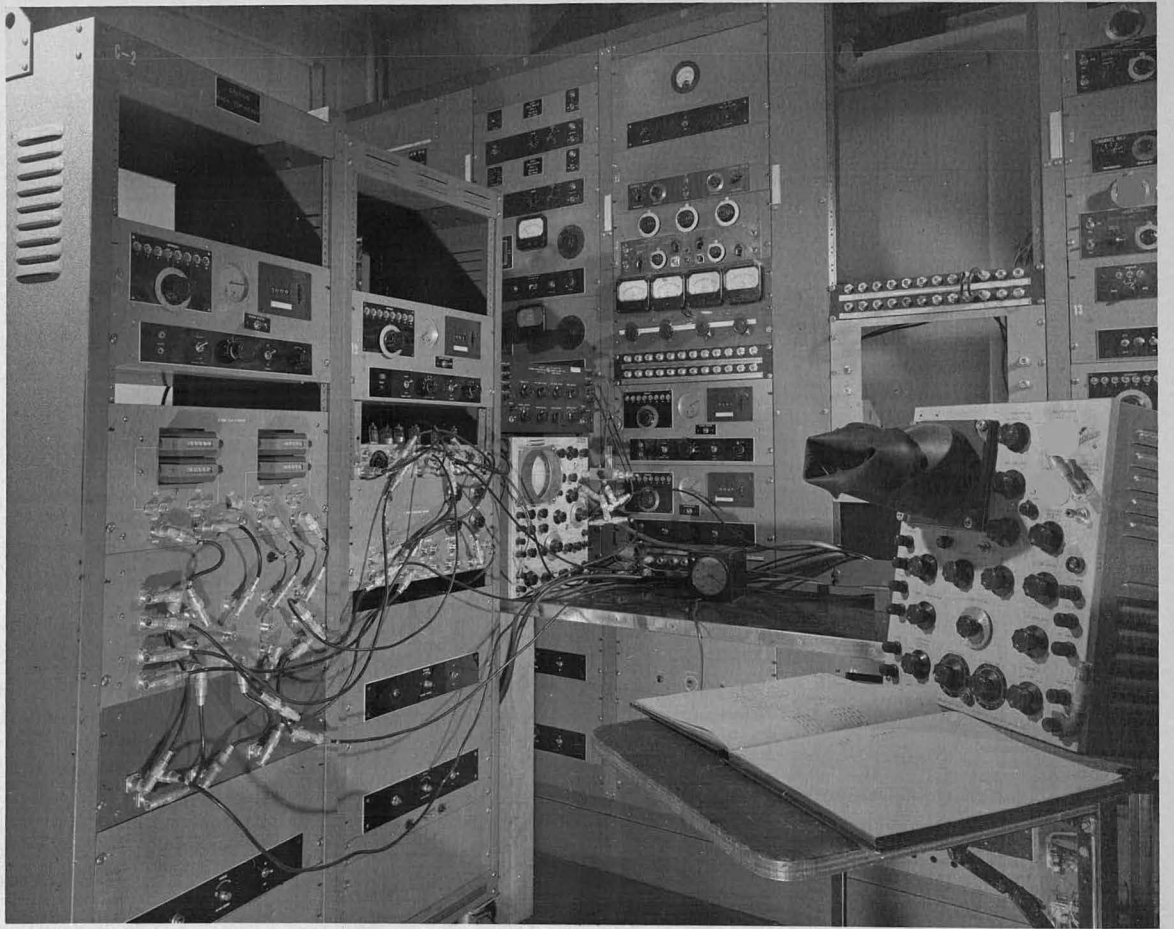
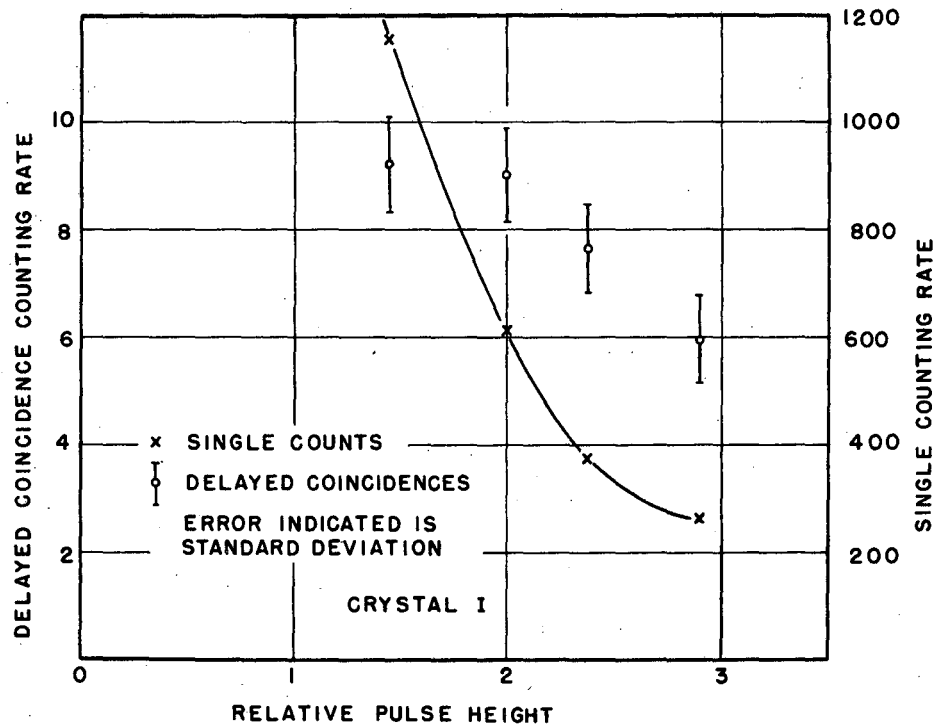
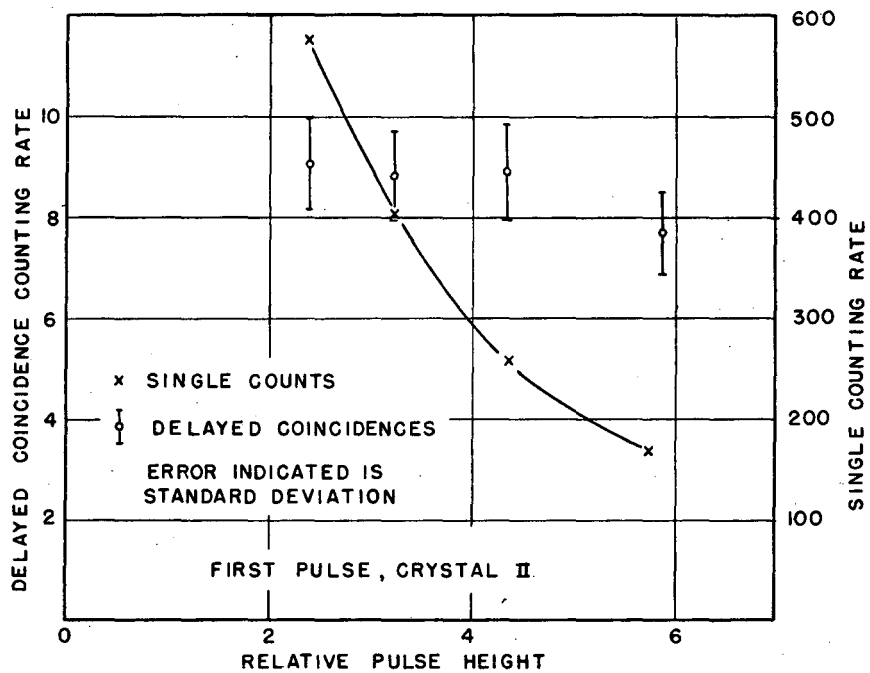


FIG. 7
ELECTRONIC EQUIPMENT



MESON COUNTING RATE AND COUNTING RATE OF PULSES FROM CRYSTAL I AS A FUNCTION OF CHANNEL I GAIN. MU 255

FIG. 8

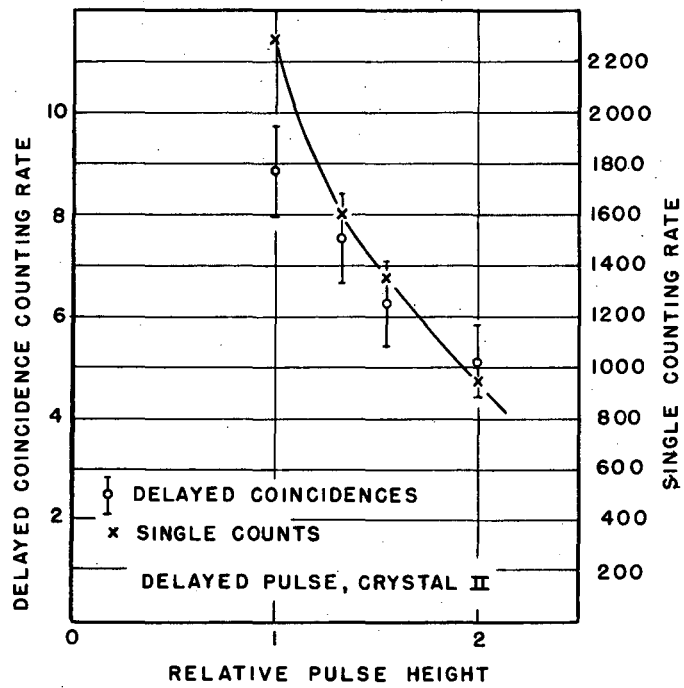


MESON COUNTING RATE AND COUNTING RATE OF FIRST PULSE FROM CRYSTAL II AS A FUNCTION OF CHANNEL II A GAIN.

FIG. 9

MU 254

MU 253



MESON COUNTING RATE AND COUNTING RATE OF 2nd PULSE FROM CRYSTAL II AS A FUNCTION OF CHANNEL II B GAIN.

FIG. 10

14496-1

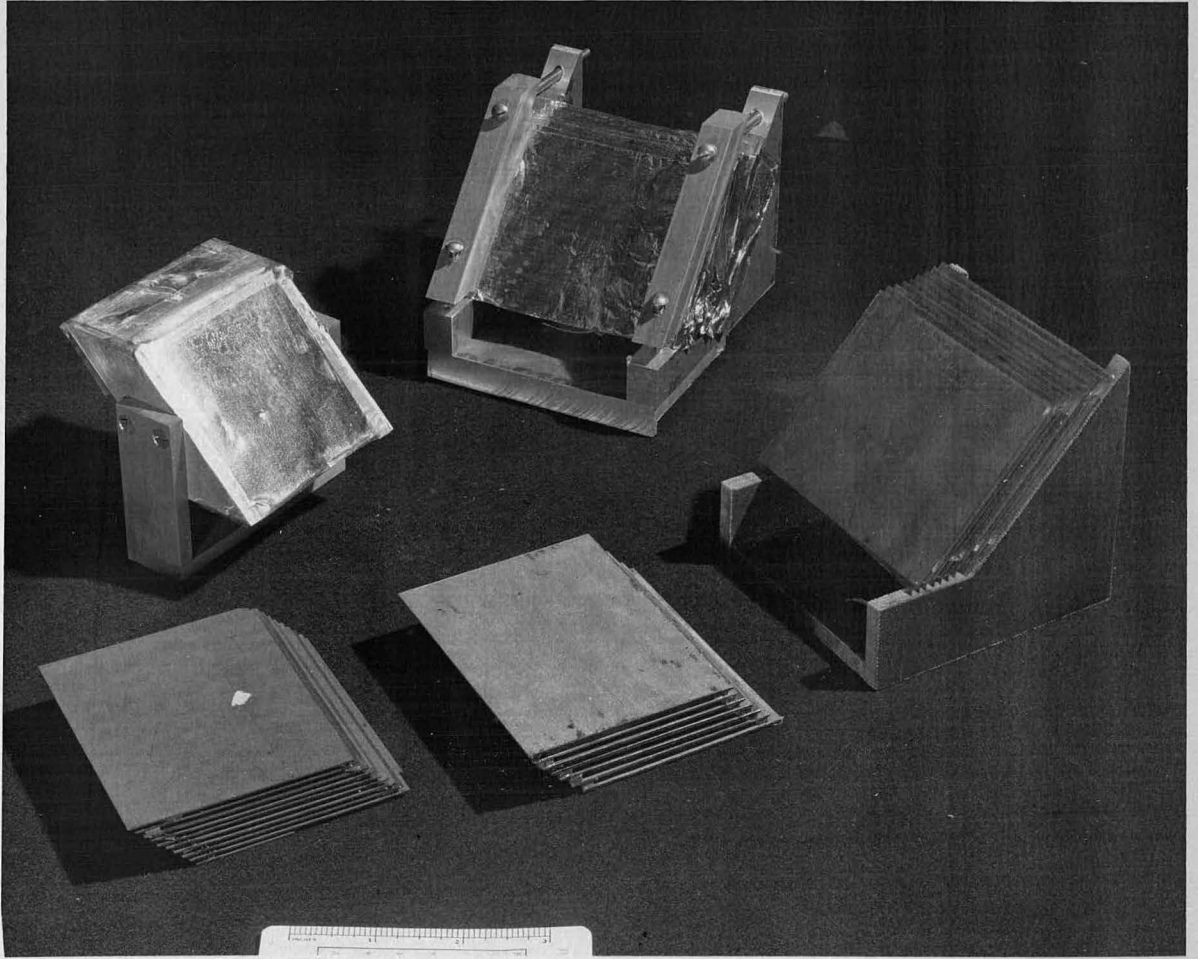


FIG. II
TARGETS

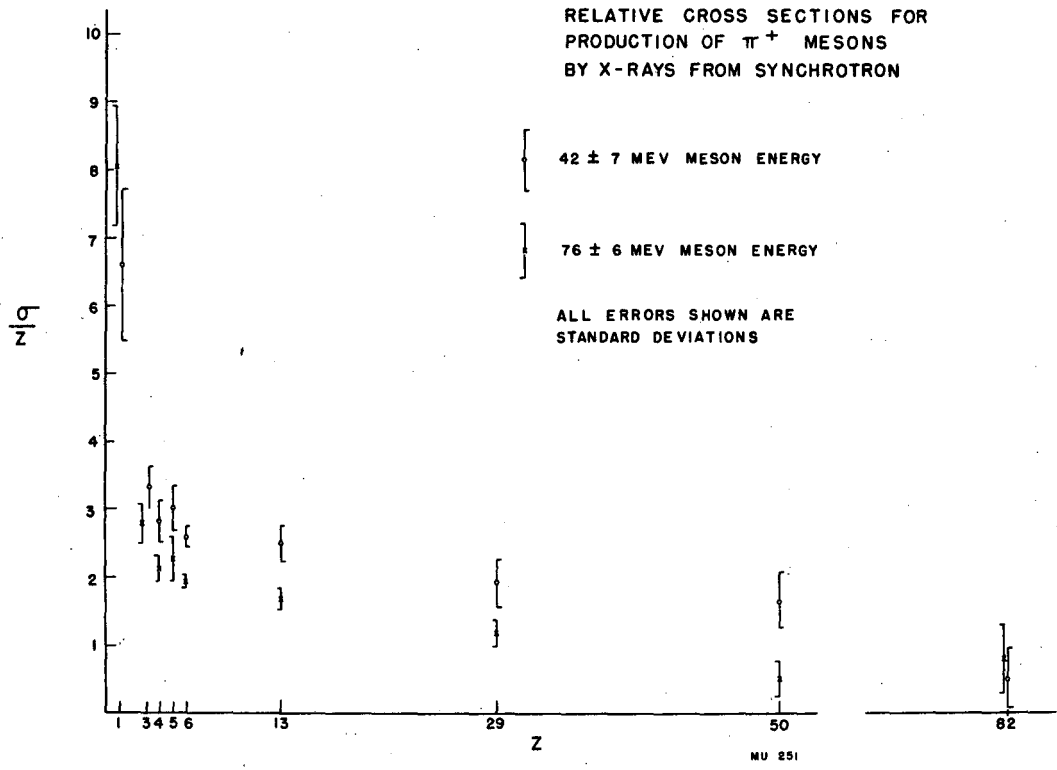


FIG 12

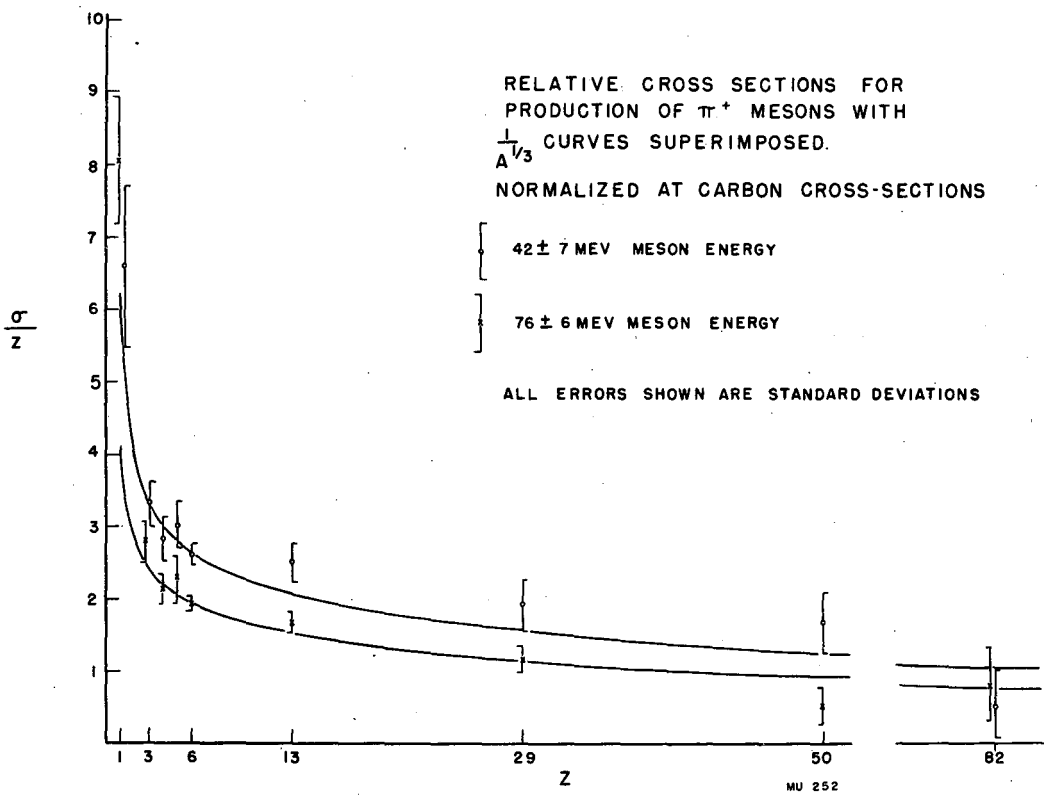


FIG. 13